Molecular Cell
Article

BAX Inhibitor-1 Is a Negative Regulator of the ER Stress Sensor IRE1α

Fernanda Lisbona,[1,2] Diego Rojas-Rivera,[1,2] Peter Thielen,[4] Sebastian Zamorano,[1,2] Derrick Todd,[4,5] Fabio Martinon,[4] Alvaro Glavic,[3] Christina Kress,[6] Jonathan H. Lin,[7,8] Peter Walter,[7,8] John C. Reed,[6] Laurie H. Glimcher,[4,5,*] and Claudio Hetz[1,2,4,*]

[1]Institute of Biomedical Sciences, FONDAP Center for Molecular Studies of the Cell
[2]Millennium Nucleus for Neural Morphogenesis
[3]Center for Genomics of the Cell, Department of Biology, Faculty of Sciences
University of Chile, Santiago, Chile
[4]Department of Immunology and Infectious Diseases, Harvard School of Public Health, Boston MA 02115, USA
[5]Department of Medicine, Harvard Medical School, Boston, MA 02115, USA
[6]Burnham Institute for Medical Research, La Jolla, CA 92037, USA
[7]Howard Hughes Medical Institute
[8]Department of Biochemistry and Biophysics
University of California at San Francisco, San Francisco, CA 94158, USA
*Correspondence: lglimche@hsph.harvard.edu (L.H.G.), chetz@hsph.harvard.edu (C.H.)
DOI 10.1016/j.molcel.2009.02.017

SUMMARY

Adaptation to endoplasmic reticulum (ER) stress depends on the activation of an integrated signal transduction pathway known as the unfolded protein response (UPR). Bax inhibitor-1 (BI-1) is an evolutionarily conserved ER-resident protein that suppresses cell death. Here we have investigated the role of BI-1 in the UPR. BI-1 expression suppressed IRE1α activity in fly and mouse models of ER stress. BI-1-deficient cells displayed hyperactivation of the ER stress sensor IRE1α, leading to increased levels of its downstream target X-box-binding protein-1 (XBP-1) and upregulation of UPR target genes. This phenotype was associated with the formation of a stable protein complex between BI-1 and IRE1α, decreasing its ribonuclease activity. Finally, BI-1 deficiency increased the secretory activity of primary B cells, a phenomenon regulated by XBP-1. Our results suggest a role for BI-1 in early adaptive responses against ER stress that contrasts with its known downstream function in apoptosis.

INTRODUCTION

A number of conditions interfere with oxidative protein-folding processes in the endoplasmic reticulum (ER) lumen (Ron and Walter, 2007), leading to a cellular condition referred to as "ER stress." Adaptation to ER stress is mediated by engagement of the unfolded protein response (UPR), an integrated signal transduction pathway that transmits information about protein-folding status in the ER lumen to the cytosol and nucleus to increase protein-folding capacity. Conversely, cells undergo apoptosis if these mechanisms of adaptation and survival are insufficient to handle the unfolded protein load.

Expression of the UPR transcription factor X-box-binding protein-1 (XBP-1) is essential for the proper function of plasma B cells (Reimold et al., 2001; Iwakoshi et al., 2003), exocrine cells of pancreas, and salivary glands (Lee et al., 2005) and for liver lipogenesis (Lee et al., 2008). Active XBP-1 is generated by the direct processing of its mRNA by the ER stress sensor IRE1α, an ER resident Ser/Thr protein kinase and endoribonuclease (Calfon et al., 2002; Lee et al., 2002). This unconventional splicing event leads to a shift in the codon reading frame, resulting in the expression of an active transcription factor termed XBP-1s that controls genes related to protein quality control, ER translocation, glycosylation, and ER/Golgi biogenesis (Shaffer et al., 2004; Lee et al., 2003a; Acosta-Alvear et al., 2007). In addition, IRE1α operates by the formation of a complex signaling platform at the ER membrane through the binding of adaptor proteins, controlling the activation the c-Jun N-terminal kinase (JNK), ERK, and NF-κB pathways (reviewed in Hetz and Glimcher, 2008b).

IRE1α activity is specifically regulated by different factors including the phosphatase PTP-1B (Gu et al., 2004), ASK1-interacting protein 1 (AIP1) (Luo et al., 2008), and some members of the BCL-2 protein family (Hetz et al., 2006). The BCL-2 family is a group of evolutionarily conserved regulators of cell death composed of both anti- and proapoptotic members that operate at the mitochondrial membrane to control caspase activation (Danial and Korsmeyer, 2004). We recently described a function for the proapoptotic BCL-2 family members BAX and BAK at the ER where they regulate the amplitude of IRE1α signaling by modulating its activation possibly by a physical interaction (Hetz et al., 2006). These findings suggested a role for BCL-2 family members as accessory factors for the instigation of certain UPR signaling events. It is unknown whether or not other apoptosis-related components regulate the UPR.

A recent study suggested that the IRE1α pathway may be modulated by additional proteins such as BAX inhibitor-1 (BI-1) (Bailly-Maitre et al., 2006). Under ischemic conditions, BI-1-deficient mice displayed increased expression of XBP-1 s in the liver

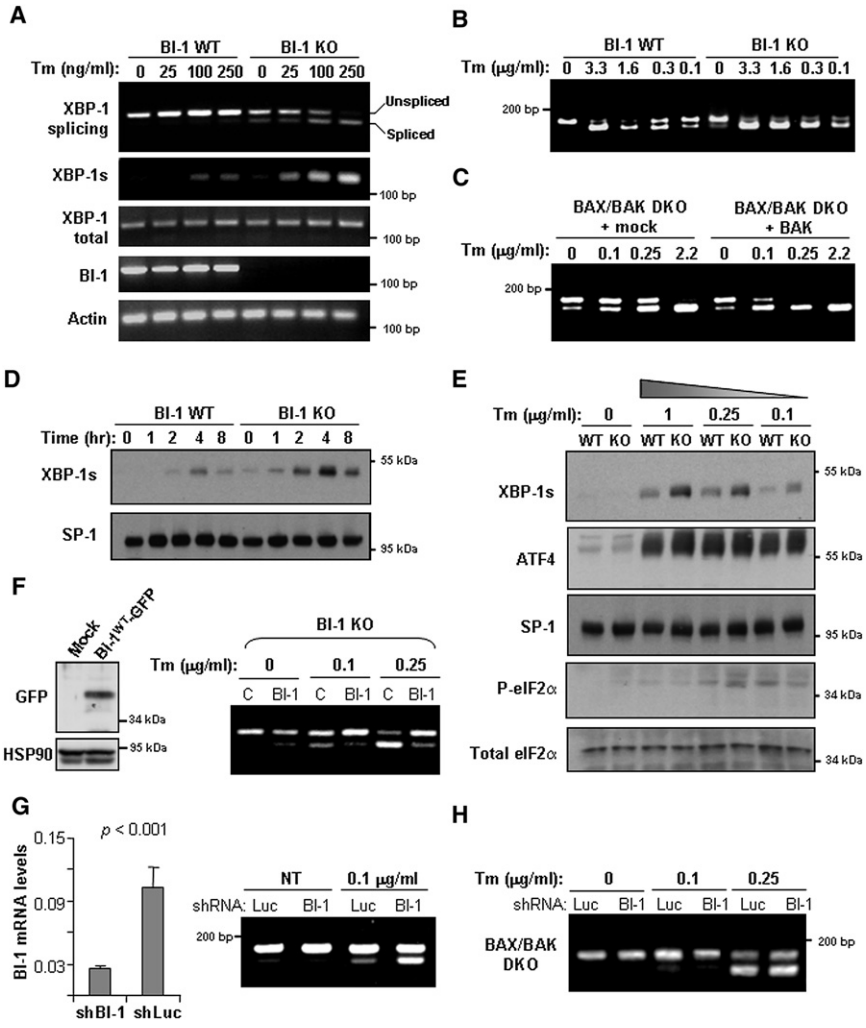

Figure 1. BI-1 Negatively Regulates IRE1α Signaling

(A) BI-1 KO and control MEFs were treated with indicated concentrations of Tm for 2.5 hr, and levels of XBP-1 mRNA splicing were determined in total cDNA by RT-PCR. Spliced and unspliced PCR fragments are indicated. In addition, total levels of XBP-1, spliced XBP-1, and actin mRNA were determined by using RT-PCR.

(B) BI-1 KO and control MEFs were treated with indicated concentrations of Tm for 2.5 hr and levels of XBP-1 mRNA splicing determined. Data presented are representative of at least ten independent experiments.

(C) BAX and BAK DKO MEFs were reconstituted with a BAK retroviral expression vector or empty vector (mock). After 48 hr, the levels of XBP-1 splicing were determined after treatment with indicated concentrations of Tm. Data are representative of three independent experiments.

(D) BI-1 WT and KO cells were treated with 100 ng/ml Tm for indicated time points, and the levels of XBP-1 s were determined in nuclear extracts by western blot analysis. The levels of SP-1 were used as internal control.

(E) In parallel, BI-1 WT and KO cells were treated with indicated concentrations of Tm for 4 hr, and then the expression levels of XBP-1 s, ATF4, and SP1 were determined in nuclear extracts. In addition, the levels of phospho-eIF2α, and eIF2α were determined by western blot in total cell extracts.

(F) BI-1 KO MEFs were reconstituted with a retroviral expression vector encoding a BI-1^{WT}-EGFP fusion protein (BI-1) and then XBP-1 mRNA splicing measured by RT-PCR after treatment with different doses of Tm for 2.5 hr. C, control BI-1 KO cells. (Left panel) BI-1-EGFP and HSP90 expression were determined by western blot.

(G) WT MEFs were transduced with lentiviral vectors expressing shRNA against the *bi-1* (shBI-1) or *luciferase* (shLuc) mRNA and levels of XBP-1 mRNA splicing determined by RT-PCR in cells treated with 100 ng/ml Tm for 2.5 hr. As control, total BI-1 mRNA levels were determined by real-time PCR. Mean and standard deviation are presented. P value was calculated by using Student's t test.

(H) In parallel, BAX and BAK DKO cells were transduced with shRNA against BI-1 mRNA or *luciferase* (Luc) and analyzed as described in (G).

and kidney (Bailly-Maitre et al., 2006). However, the mechanism underlying this phenotype was not investigated. BI-1 is a six transmembrane-containing protein functionally related to the BCL-2 family of proteins and is primarily located in the ER membrane (Xu and Reed, 1998). BI-1 has no obvious homology with BCL-2-related proteins, yet it physically interacts with different members of this family, such as BCL-2 and BCL-X_L (Xu and Reed, 1998; Chae et al., 2004). In mammalian cells, BI-1 is an antiapoptotic protein that protect cells against many different intrinsic death stimuli (Xu and Reed, 1998), including ER stress, among others (Chae et al., 2004). Further studies revealed that BI-1 is well conserved in yeast, plants, viruses, and many other organisms (Chae et al., 2003; Huckelhoven, 2004) in which its function remains poorly explored. Here we investigated the possible role of BI-1 in the UPR. Overall, our results reveal a function for BI-1 by which it negatively modulates the IRE1α/XBP-1 pathway. Our findings suggest a model wherein the expression of anti- and proapoptotic proteins at the ER membrane determines the amplitude of UPR responses.

RESULTS

BI-1 Deficiency Increases XBP-1 mRNA Splicing

Although IRE1α is the most evolutionarily conserved pathway of the UPR, little is known about its regulation. To define the possible regulation of IRE1α by BI-1, we determined the levels of *xbp-1* mRNA splicing using two different methods in BI-1 knockout (BI-1 KO) murine embryonic fibroblasts (MEFs). We titrated down the dose of the experimental ER stressor tunicamycin (Tm) to a point at which wild-type (WT) MEFs displayed only minimal processing of XBP1 mRNA (Figure 1A). Notably, under these conditions, BI-1 KO MEFs displayed pronounced splicing of the XBP1 mRNA. The inhibitory effects of BI-1 on XBP-1 mRNA splicing were minor at very high concentrations

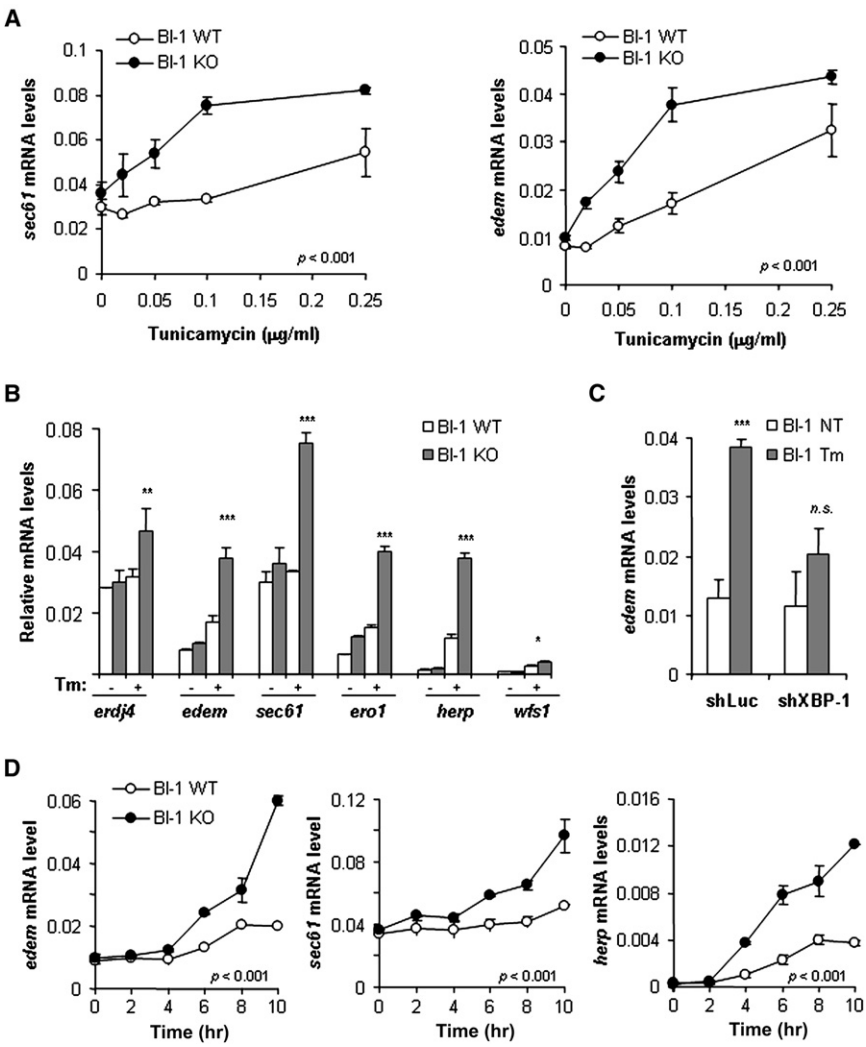

Figure 2. Increased UPR Responses in BI-1-Deficient Cells

(A) BI-1 WT and KO MEFs were treated with indicated concentrations of Tm for 8 hr, and the mRNA levels of the XBP-1 target genes Sec61 and EDEM were determined by real-time PCR.

(B) A panel of UPR target genes was analyzed by real-time PCR in BI-1 WT and KO cells treated with 100 ng/ml of Tm for 8 hr. P values were calculated with Student's t test comparing BI-1 WT and KO cells treated with Tm (*p = 0.05, **p = 0.01, ***p < 0.001).

(C) As control, the mRNA levels of EDEM were determined in BI-1 KO cells expressing shRNA against XBP-1 or control shRNA (luciferase).

(D) The mRNA levels of EDEM, Sec61, and HERP were determined at indicated time points in cells treated with 100 ng/ml Tm. In (A) and (B), p values were calculated by two-way ANOVA to compare the effects of BI-1 ablation on UPR target gene upregulation. In experiments (A)–(D), data represent average and standard deviation representative of three experiments.

of Tm (>1.6 μg/ml, Figure 1B), indicating that BI-1 is a modulator of IRE1α activity. Consistent with our previous findings (Hetz et al., 2006), low doses of Tm treatment revealed positive modulation of IRE1α activity by the proapoptotic molecule BAK (Figure 1C). In addition, we were able to validate these results by using other ER-stress-inducing agents, such as brefeldin A (inhibits ER to Golgi trafficking) and thapsigargin (blocks the ER-calcium pump SERCA) (see Figure S1 available online).

In agreement with the increased XBP-1 mRNA splicing observed above, enhanced expression of XBP-1s protein was observed in BI-1 cells undergoing ER stress when compared with control BI-1 WT cells (Figures 1D and 1E). BI-1 deficiency did not significantly affect the expression of IRE1-independent events such as ATF4 expression and eIF2α phosphorylation (Figure 1E), suggesting that BI-1 specifically affects UPR events initiated by IRE1α and not by the stress sensor PERK. We confirmed our results by reconstituting BI-1 KO cells with a human BI-1, which drastically decreased the levels of XBP-1 mRNA splicing (Figure 1F).

In order to rule out possible compensatory effects associated with BI-1 deficiency, we targeted BI-1 mRNA with small hairpin RNA (shRNA) and lentiviral vectors. This strategy led to an ~75% decrease in BI-1 mRNA levels (Figure 1G). BI-1 knockdown cells displayed increased levels of XBP-1 mRNA splicing when compared with control cells (Figure 1G). Interestingly, knockdown of BI-1 in BAX/BAK DKO cells did not restore the normal levels of XBP-1 mRNA splicing, suggesting that BI-1 operates upstream of BAX and BAK in the control of the IRE1α/XBP-1 pathway (Figure 1H). To complement these experiments, we analyzed the expression levels of BI-1 mRNA, the stability of ectopically expressed BI-1, and its subcellular distribution under ER stress conditions. No alteration in the levels of BI-1 expression or its distribution pattern was observed under these conditions (Figure S2).

Increased Upregulation of XBP-1s Target Genes in BI-1 KO Cells

Previous work has demonstrated that XBP-1s regulates the expression of ER-stress-induced genes that promote folding, degradation of misfolded ER proteins through the ER-associated degradation (ERAD) pathway and genes involved in the translocation of proteins into the ER. XBP-1s target genes were previously defined in MEFs by our laboratory using cDNA microarray analysis (Lee et al., 2003a) and include chaperones (i.e., *ERdj4*), ERAD-related genes (i.e., *edem* and *herp*), genes involved in protein translocation into the ER (i.e., *Sec61*), and many others (Lee et al., 2003a; Shaffer et al., 2004). To define the impact of BI-1 on UPR adaptive responses, we determined the levels of XBP-1s target genes in BI-1-deficient cells by real-time PCR. Dose-response experiments demonstrated an increased upregulation of the mRNAs encoding Sec61 and EDEM in BI-1 KO cells when compared with control cells (Figure 2A). Analysis

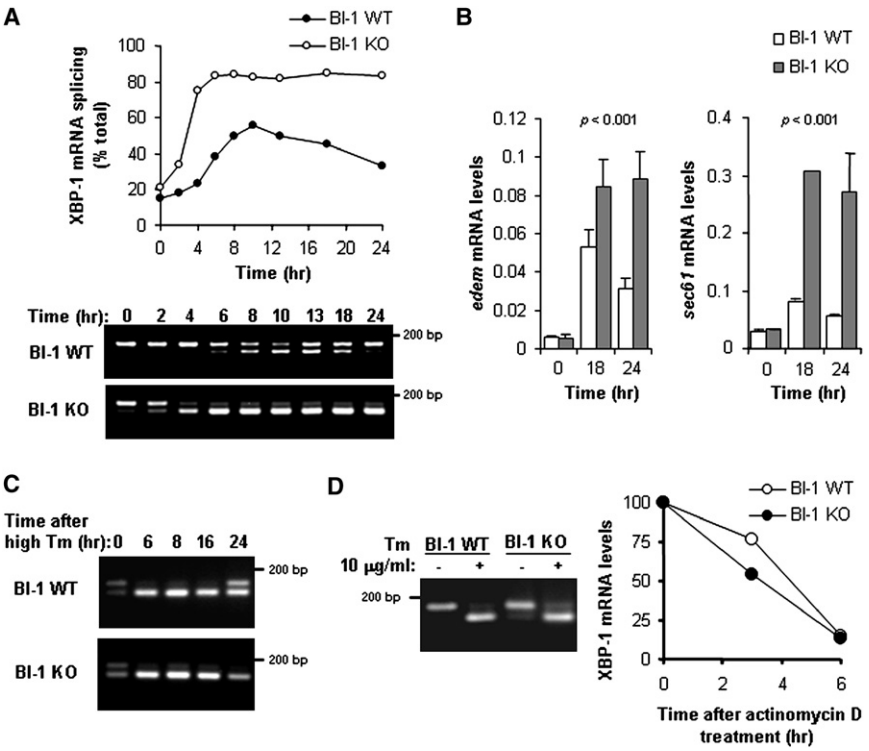

Figure 3. Delayed Inactivation of XBP-1 mRNA Splicing in BI-1-Deficient Cells

(A) (Lower panel) XBP-1 mRNA splicing was monitored over time in BI-1 WT and KO cells treated with 100 ng/ml Tm. (Upper panel) Quantification of the percentage of XBP-1 mRNA splicing was calculated after the densitometric analysis.

(B) XBP-1 target genes *edem* and *sec61* were evaluated in BI-1 WT and KO MEFs after 18 and 24 hr of treatment with 100 ng/ml Tm by using real-time PCR. P values were calculated by two-way ANOVA to compare the effects of BI-1 ablation on UPR target gene upregulation.

(C) BI-1 WT and KO cells were treated for 2 hr with 1 μg/ml of Tm and washed three times with PBS. Then mRNA splicing was evaluated by RT-PCR during the recovery period at indicated time points.

(D) BI-1 WT and KO cells were treated with 10 μg/ml of Tm for 3 hr to trigger complete XBP-1 mRNA splicing. Then cells were treated with 3 μg/ml actinomycin D to block transcription, and the decay of XBP-1 mRNA was followed over time by real-time PCR of total cDNA and normalized with the XBP-1 mRNA levels of control cultures not treated with actinomycin D.

of a broad panel of XBP-1s target genes in cells treated with 100 ng/ml Tm revealed a marked activation of the UPR in BI-1 KO MEFs (Figure 2B and Figure S1C). As control, we knocked down XBP-1 with shRNA in BI-1 KO cells and then assessed the mRNA levels of *edem* in cells undergoing ER stress, observing a decreased upregulation when compared with control cells (Figures 2C and 4A), similar to the phenotype of XBP-1 KO MEFs (Figure S3A). Detailed time course experiments indicated a more rapid and more pronounced upregulation of XBP-1s target genes in BI-1 KO cells (Figure 2D).

BI-1 Expression Regulates the Inactivation of IRE1α/XBP-1 Signaling

We have recently reported that XBP-1 mRNA splicing levels decline after prolonged ER stress (Lin et al., 2007). Here we corroborated these observations in BI-1 WT cells, observing a decrease in the levels of splicing around 18 hr of Tm treatment (Figure 3A). Surprisingly, we observed a sustained maintenance of XBP-1 mRNA splicing in BI-1-deficient cells, even after 24 hr of treatment, suggesting that BI-1 may be involved in the inactivation of IRE1α signaling (Figure 3A). These effects correlated well with the prolonged upregulation of EDEM and Sec61 mRNA up to 24 hr after Tm treatment in BI-1-deficient cells (Figure 3B).

To further evaluate the possible participation of BI-1 in the inactivation of IRE1α, we treated BI-1 WT and KO cells for only 2 hr with high doses of Tm to trigger almost full XBP-1 mRNA splicing in both cell types. Tm-containing media was then washed out and XBP-1 mRNA splicing monitored during the recovery period. Under these experimental conditions, XBP-1 mRNA levels decreased by half in BI-1 WT cells by 24 hr posttreatment, whereas complete retention of XBP-1 splicing was still observed in BI-1 KO cells (Figure 3C). Taken together, these results suggest that BI-1 regulates the amplitude of IRE1α signaling possibly by downregulating its activity. In control experiments, we monitored XBP-1 mRNA stability in BI-1 WT and KO cells undergoing ER stress. No significant differences in the decay of XBP-1 mRNA were observed in either cell type (Figure 3D).

Dual Role of BI-1 in the Regulation of UPR Signaling and Downstream Apoptosis

Activation of the IRE1α/XBP-1 pathway confers cellular protection in adaptation to ER stress (Lin et al., 2007). To determine the consequences of BI-1-regulated XBP-1 mRNA splicing on survival and adaptation to ER stress, we introduced IRE1α and XBP-1 shRNAs into BI-1 KO and control cells (Figure 4A) and then assessed the effects on cell survival. As shown in Figure 4B, inhibition of XBP-1s expression in BI-1 KO cells further enhanced their susceptibility to ER stress, as evidenced by increased cell death. Interestingly, when experiments were performed with 100 ng/ml of Tm, the effects of knocking down XBP-1 on cell viability were only evident in BI-1-deficient cells and not control cells (Figure 4B), consistent with the dramatic differences observed in the levels of XBP-1 mRNA splicing under these conditions (Figure 1A). At high doses of Tm, the protective effects of XBP-1 expression were also observed in BI-1 WT cells (Figure 4B). Similar results were obtained when the levels of IRE1α were reduced with shRNA in BI-1 KO cells (Figure 4C). Thus, the previously described increased susceptibility of BI-1-deficient cells to ER-stress-induced apoptosis (Figures S3B and S3C) is a combination of the balance between its

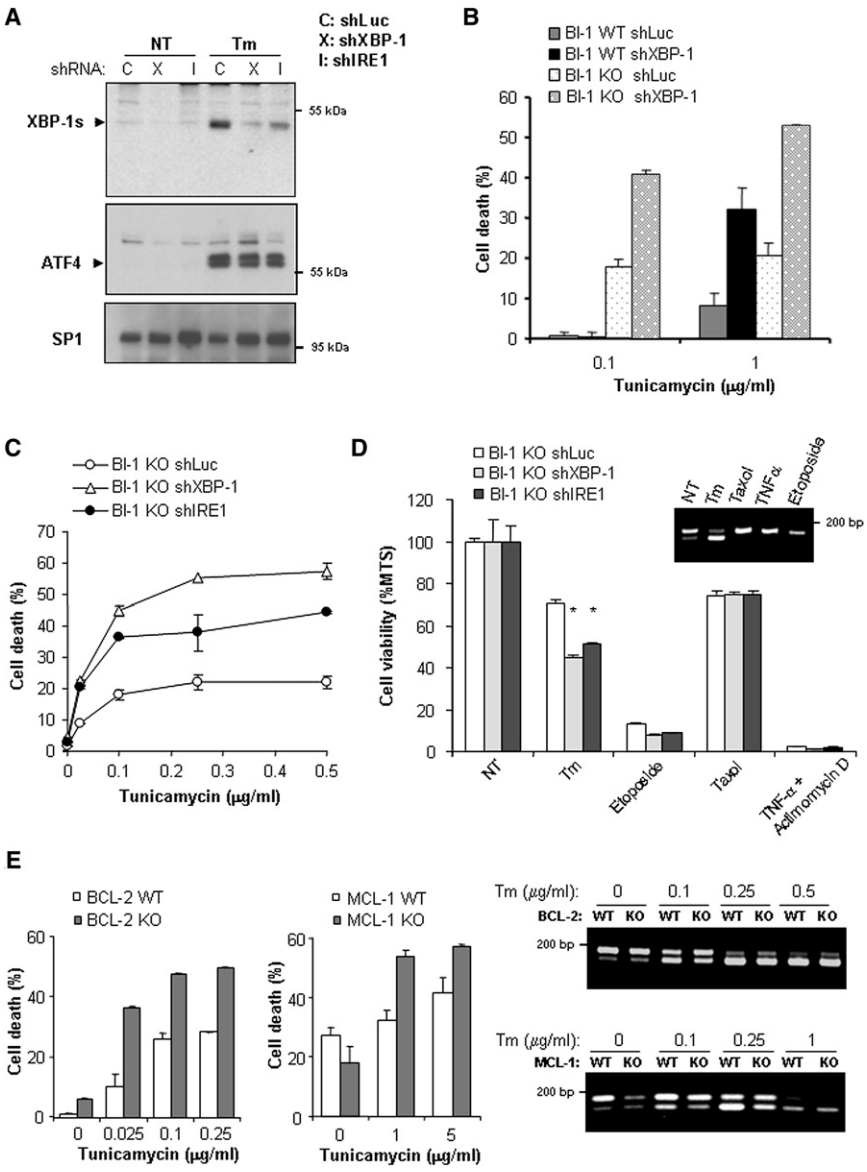

Figure 4. BI-1 Regulates Prosurvival Responses Dependent on IRE1α/XBP-1

(A) BI-1 KO MEFs were stably transduced with lentiviral vectors expressing shRNA against the *xbp-1*, *ireα* (shXBP-1 and shIRE1α), or *luciferase* (shLuc) mRNA, and levels of XBP-1 s were determined by western blot in total nuclear extracts. As controls, ATF4 and SP-1 levels were determined.

(B) BI-1 WT and KO MEFs were stably transduced with lentiviral vectors expressing shRNA against the *xbp-1* (shXBP-1) or *luciferase* (shLuc) mRNA and then treated with 0.1 or 1 μg/ml of Tm for 24 hr, and cell death was determined by PI staining and FACS analysis.

(C) BI-1 KO shIRE1, shXBP-1, and shLuc cells were treated with indicated concentrations of Tm for 24 hr, and cell death was determined by PI staining and FACS analysis.

(D) BI-1 KO cells transduced with indicated shRNA constructs were exposed to 0.1 μg/ml Tm, 40 μM etoposide, and 50 ng/ml TNF-α together with 1 μg/ml actinomycin D or 10 μM taxol for 24 hr, and cell viability was analyzed by the MTS assay. (Inset) The levels of XBP-1 splicing were assessed in WT MEFS after similar treatments for 3 hr. Average and standard deviations represent three determinations. *$p < 0.001$ using Student's t test.

(E) The levels of XBP-1 splicing (right panels) and cell death (left panels) were assessed in BCL-2 WT and KO MEFs, or MCL-1 WT and KO MEFs treated with indicated concentrations of Tm for 2.5 hr (splicing) or 24 hr (cell viability, PI staining, and FACS analysis).

downstream control of the apoptosis machinery and the early regulation of prosurvival signals mediated by IRE1α/XBP-1 activation.

No effects were observed on the viability of XBP-1 or IRE1α knockdown cells when they were exposed to non-ER-stress-related challenges, including TNFα (death receptors), paclitaxel (Taxol, destabilize cytoskeleton), or etoposide (DNA damage) (Figure 4D). Consistent with this observation, these drugs did not induce XBP-1 splicing (Figure 4D, inset). As additional controls, we analyzed levels of XBP-1 mRNA splicing in MEFs deficient in the antiapoptotic genes MCL-1 or BCL-2. We did not observe any significant increase in XBP-1 splicing in these cells, despite a clear increase in susceptibility to ER-stress-dependent cell death (Figure 4E). Hence an augmented susceptibility to cell death does not by itself increase XBP-1 mRNA splicing activity.

BI-1 Forms a Protein Complex with IRE1α

The activation of IRE1α requires dimerization, which then triggers its autophosphorylation and RNase activity. We predicted that the immunoprecipitation (IP) of IRE1α would promote its dimerization and activation in the absence of an ER stressor. We developed an assay to monitor the RNase activity of IRE1α in vitro purified from MEFs by the IP of an N-terminal HA-tagged form of IRE1α (IRE1α-HA) followed by the incubation of the extracted protein complexes with a total mRNA mixture in the presence of ATP to trigger XBP-1 mRNA splicing. IRE1α-containing IP protein complexes from BI-1 KO cells were more active than IRE1α extracted from control cells (Figure 5A). These data suggest that the expression of BI-1 negatively modulates the RNase activity of IRE1α in our cell-free assay. We also analyzed the rate of IRE1α phosphorylation in BI-1 KO cells undergoing ER stress. BI-1 KO cells stimulated with 100 ng/ml of Tm for 30 min showed a characteristic phosphorylation shift of IRE1α that was absent in control cells (Figure S4A).

Based on the results of our in vitro splicing assay, we searched for a physical interaction between BI-1 and IRE1α. Coimmunoprecipitation (coIP) experiments using lysates from cells

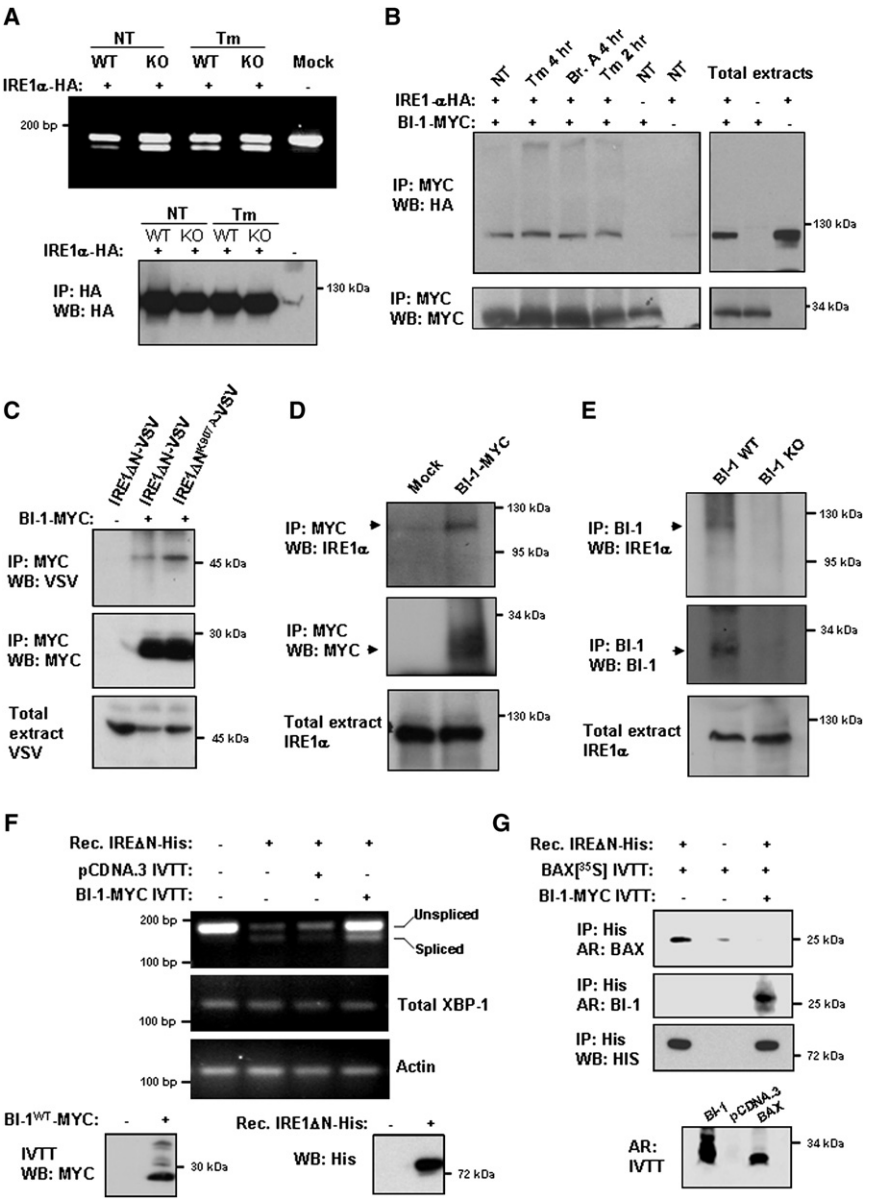

Figure 5. BI-1 Forms a Protein Complex with IRE1α and Regulates Its Endoribonuclease Activity

(A) BI-1 WT and KO MEFs expressing HA-tag IRE1α (IRE1α-HA) were treated with 100 ng/ml Tm or left untreated. IRE1α-HA was immunoprecipitated (IP) and then incubated with total brain mRNA (substrate). After 30 min, mRNA was re-extracted, and the levels of XBP-1 mRNA splicing were determined by RT-PCR. (Bottom panel) The levels of IRE1α-HA expression were determined by western blot of the immunoprecipitates.

(B) 293T cells were cotransfected with expression vectors for BI-1-MYC and IRE1α-HA. After 48 hr, cells were treated with 0.5 μg/ml Tm or 20 μM brefeldin A (Bref. A) for indicated time points, and then the coprecipitation of MYC-BI-1 with IRE1α-HA was evaluated by IP and western blot.

(C) 293T cells were transfected with BI-1-MYC or an IRE1α inactive mutant (K907A) in the presence of VSV-tagged IRE1α lacking its ER luminal domain (IRE1ΔN-VSV) and then IP and western blot analysis performed as in (B).

(D) HEK cells were transiently transfected with a BI-1-MYC expression vector or empty pCDNA.3 vector. After 48 hr, BI-1-MYC was immunoprecipitated, and its association with endogenous IRE1α was assessed by western blot.

(E) Endogenous BI-1 was immunoprecipitated from MEFs cells, and its association with endogenous IRE1α was determined by western blot analysis. As a control experiment, IP was performed from BI-1 KO cells.

(F) The endoribonuclease activity of recombinant (rec.) IRE1ΔN-HIS was monitored in vitro using the conditions described in the Supplemental Experimental Procedures. IVTT BI-1-MYC or control IVTT from empty vector (pCDNA.3) was preincubated with IRE1ΔN-HIS for 1 hr at 30°C, and then total mRNA was added to the reaction and incubated for 1 hr. Then the ribonuclease activity of IRE1α was analyzed by RT-PCR by using regular XBP-1 mRNA splicing primers, evidenced as decreased PCR product of the non-spliced fragment. Total XBP-1 mRNA and actin were monitored as control. (Lower panel) Western blot analysis of IVTT BI-1-MYC and IRE1ΔN-HIS is shown.

(G) IVTT BI-1 was incubated with recombinant IRE1ΔN-HIS in the presence or absence of IVTT BAX Met-^{35}S labeled (upper panel). Then IRE1ΔN-HIS was pulled down, and its association with radiolabel BAX was determined by electrophoresis and autoradiograph (AR). As control, IRE1ΔN-HIS levels were determined by western blot. To address the binding of BI-1 to IRE1, IVTT BI-1 Met-^{35}S labeled was used with nonlabeled BAX in the same experimental conditions. (Bottom panel) Met-^{35}S-labeled BI-1, BAX, and mock (pCDNA.3) were analyzed by electrophoresis and autoradiograph.

cotransfected with IRE1α-HA and MYC-tagged BI-1 showed an association between both proteins (Figure 5B). BI-1 interaction required the cytosolic C-terminal region of IRE1α, which encodes the kinase and endoribonuclease domains (Figures 5C and 6B). Finally, the interaction of BI-1 with IRE1α was not altered in cells undergoing ER stress triggered by Tm or brefeldin A treatments (Figure 5B), indicating constitutive binding of BI-1 and IRE1α under resting conditions. In agreement with this result, BI-1 associated equally well in coIP experiments with an inactive IRE1α mutant (K907A) and WT IRE1α (Figure 5C). More importantly, we were able to confirm our experiments by monitoring the interaction between ectopically expressed BI-1-MYC and endogenous IRE1α in human cells (Figure 5D). We were also successful in detecting a physical association between endogenous BI-1 and endogenous IRE1α (Figure 5E).

We next tested the possible effects of BI-1 on the activity of IRE1α. We established an in vitro assay to monitor the endoribonuclease activity of purified IRE1α. The cytosolic His-tag version of human IRE1α (IRE1ΔNα-HIS) was expressed and purified from insect cells, since they express a BAX and BI-1 homolog and because this mutant of IRE1α adopts an active dimeric state (data not shown). Then, purified IRE1ΔNα-HIS was incubated

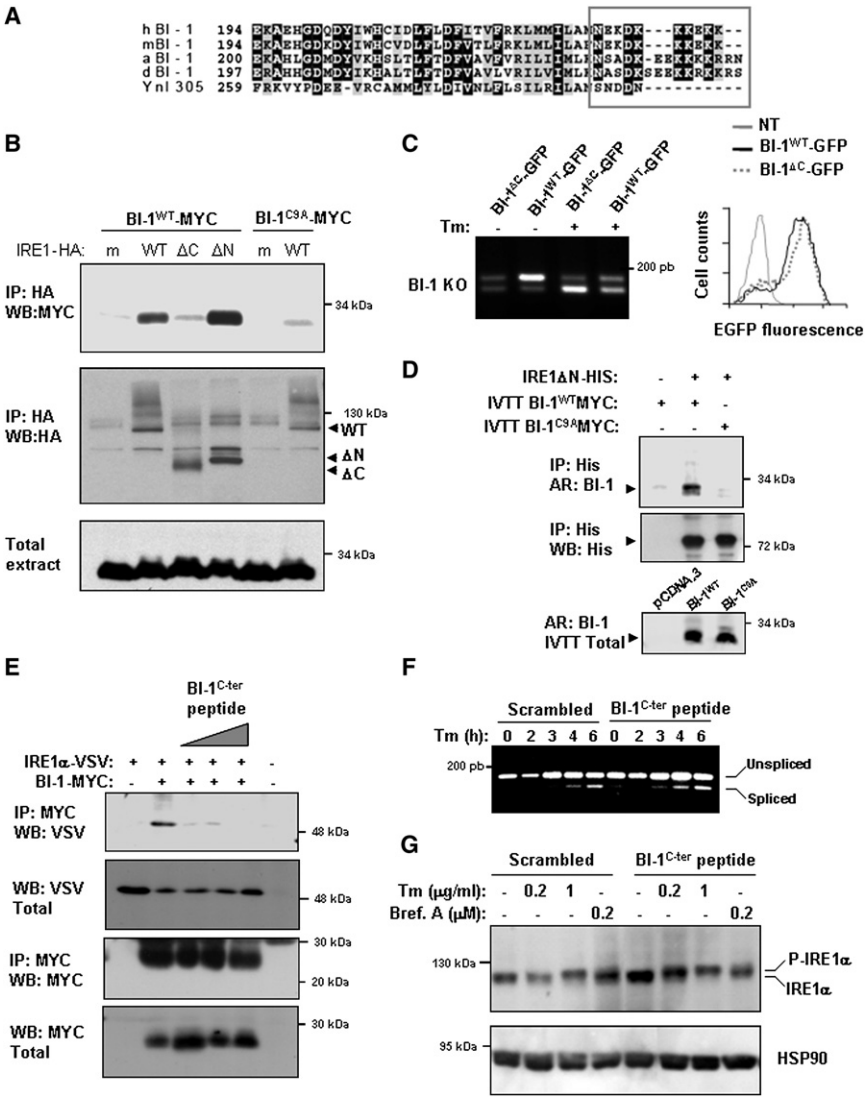

Figure 6. BI-1 Regulates IRE1α through Its Cytosolic C-Terminal Region

(A) Amino acid sequence comparison of the C-terminal region of BI-1 from different species including BI-1 from human (hBI-1), mouse (mBI-1), *Arabidopsis thaliana* (aBI-1), *Drosophila melanogaster* (dBI-1), and the putative yeast homolog YN1305c. Predicted C-terminal cytosolic domain is highlighted with a gray square.

(B) 293T cells were cotransfected with expression vectors for BI-1^{WT}-MYC or BI-1^{C9A}-MYC with IRE1α-HA (WT) or IRE1α deletion mutant of the cytosolic (ΔC), ER luminal domain (ΔN), or empty vector (m). After 48 hr, cell extracts were prepared, and IRE1α-HA was immunoprecipitated and interactions with BI-1 determined by western blot.

(C) BI-1 KO MEFs were reconstituted with expression vectors for EGFP fusion proteins of BI-1^{WT} or BI-1ΔC and then XBP-1 s mRNA levels measured by RT-PCR after treatment with different doses of Tm for 2.5 hr. (Right panel) BI-1 expression levels were analyzed by monitoring EGFP fluorescence by FACS.

(D) IVTT BI-1^{WT}-MYC and BI-1^{C9A}-MYC labeled with Met-^{35}S were incubated for 3 hr with recombinant IRE1ΔN-HIS. Then IRE1ΔN-HIS was pulled down and its association with radiolabeled BI-1 determined by electrophoresis and autoradiograph (AR). (Bottom panel) Levels of radiolabel BI-1^{WT}-MYC, BI-1^{C9A}-MYC, or mock (pCDNA.3) were compared by autoradiograph.

(E) 293T cells were cotransfected with expression vectors for BI-1-MYC and the VSV-cytosolic domain of IRE1α, and after 48 hr, BI-1-MYC was immunoprecipitated. Isolated protein complexes were incubated with increasing concentrations (10, 50, and 150 μM) of a synthetic peptide representing the C-terminal ten amino acids of BI-1 for 30 min, and IRE1α association with BI-1 measured by western blot.

(F) BI-1 WT and KO cells were treated with 10 μM BI-$1^{C\text{-}ter}$ peptide or control scrambled peptide for 2 hr, cells treated with 100 ng/ml Tm for indicated time points, and levels of XBP-1 mRNA splicing determined in total cDNA by RT-PCR.

(G) WT MEFs were pretreated with 10 μM BI-$1^{C\text{-}ter}$ peptide or scrambled peptide for 2 hr and then treated with 200 ng/ml Tm or 0.2 μM brefeldin A for 2 hr or with 1 μg/ml Tm as positive control. Then the phosphorylation shift (P-IRE1) of endogenous IRE1α was monitored by western blot. HSP90 levels were analyzed as loading control.

with a mixture of total mRNA in the presence or absence of in vitro-transcribed/translated (IVTT) BI-1. After 1 hr of incubation, mRNA was re-extracted, and the cleavage of XBP-1 mRNA in the splicing site was monitored by RT-PCR. As shown in Figure 5F, the activity of IRE1ΔN-HIS was almost completely blocked by the presence of BI-1 in the reaction. These results indicate that the effects of BI-1 on IRE1α activity can be reconstituted in vitro, suggesting a direct regulation.

We tested for possible effects of BI-1 on the binding of BAK to IRE1α. We first performed transient transfection of different combinations of IRE1α-HA, BAK, and BI-1-MYC. Coexpression of BAK and BI-1 reduced the interaction of BAK with IRE1α as compared with control (Figure S4B). Similar results were observed when the binding of BAX to the complex was tested in the same experimental system (data not shown). We have previously described that the physical association between IRE1α and BAX is recapitulated with recombinant proteins, indicating a direct interaction (Hetz et al., 2006). To monitor the binding of BI-1 to IRE1α, we first performed pull-down assays with recombinant IRE1ΔN-HIS and IVTT BI-1^{WT}. We were able to detect the formation of a protein complex between IRE1α and BI-1^{WT} in vitro (Figures 6D and 5G). Interestingly, in the same experimental system, the presence of BI-1 drastically reduced the binding of IVTT BAX to IRE1ΔN-HIS (Figure 5G), suggesting that BAX and BI-1 regulate IRE1α through related mechanisms and may compete for a common binding site. Taken together with the results shown in Figure 1H, these findings suggest that BI-1 operates upstream of BAX and BAK in the control of IRE1α inactivation. In agreement with previous findings (Xu and Reed, 1998), we did not observe a significant

interaction between BI-1 and BAX or BAK, but it associated with BCL-2 or BCL-X_L (Figures S4C–S4E).

BI-1 Regulates IRE1α through Its C-Terminal Region

Bioinformatic analysis of the BI-1 sequence failed to identify known possible protein-protein interaction or catalytic domains present in other proteins. The cytosolic C terminus of mammalian BI-1 is composed of only ten amino acids, and it is conserved in multicellular organisms (Figure 6A) and has been shown to be essential for the regulation of apoptosis (Chae et al., 2003). We expressed a BI-1 mutant in which the last nine amino acids of the protein were replaced by alanines (BI-1^{C9A}) and tested its interaction with IRE1α. As shown in Figure 6B, BI-1^{C9A} did not significantly interact with IRE1α, but it still located at the ER (Figure S5). Hence, the lack of physical association between BI-1^{C9A} and IRE1α is not due to a change in the subcellular localization of the mutant protein.

To test the role of the C-terminal region of BI-1 on IRE1α signaling, we performed reconstitution experiments in BI-1 KO cells. Ectopic expression of human BI-1 (hBI-1) reduced the levels of XBP-1 mRNA splicing in BI-1 KO cells (Figure 6C), an effect that was not observed in cells expressing mutant BI-1 where full XBP-1 mRNA splicing was still observed. To monitor the effects of the C-terminal region of BI-1 on the interaction with IRE1α, we performed pull-down assays with recombinant IRE1ΔN-HIS and IVTT BI-1^{WT} or BI-1^{C9A}. Mutation on the C-terminal region of BI-1 completely abrogated its association with IRE1ΔN-HIS (Figure 6D).

We characterized in more detail the function of the C terminus of BI-1 on the UPR. A synthetic peptide containing the last 13 amino acids of BI-1 was fused with a polyarginine tag to enhance cell permeability (BI-$1^{C\text{-}ter}$). To test the effects of the peptide on the interaction between BI-1 and IRE1α, we first immunoprecipitated the BI-1/IRE1α complex and then incubated it with different concentrations of BI-$1^{C\text{-}ter}$ for 30 min. At 150 μM, the peptide completely displaced IRE1α from BI-1^{WT}, confirming the requirement of the C terminus for its interaction with IRE1α (Figure 6E). We then assessed the activity of BI-$1^{C\text{-}ter}$ in cells treated with Tm. Treatment of cells with the C-terminal BI-1 peptide increased XBP-1-spliced mRNA (Figure 6F) and augmented the levels of *herp* mRNA when compared with a control scrambled peptide (Figure S4G). This effect was not observed in BI-1 KO MEFs (Figure S4F), indicating that the activity of the BI-$1^{C\text{-}ter}$ peptide is specific and depends on the expression of endogenous BI-1. In addition, the BI-$1^{C\text{-}ter}$ peptide did not increase XBP-1 mRNA splicing in BAX and BAK DKO cells (Figure S4H). To complement these experiments, we monitored the effects of the BI-$1^{C\text{-}ter}$ peptide on the phosphorylation of IRE1α, an event associated with its activation. BI-$1^{C\text{-}ter}$ peptide drastically increased the rate of IRE1α phosphorylation in cells treated with low doses of Tm or brefeldin A (Figure 6G). Taken together, these results reinforce the observation that BI-1 is a negative regulator of IRE1α and that this regulation occurs through the formation of a protein complex between the two proteins.

BI-1 Regulates IRE1α In Vivo in Multicellular Organisms

Homologs of hBI-1 have been identified in different species including plants such as *Arabidopsis thaliana*, invertebrate animals such as *Drosophila melanogaster* (dBI-1), the budding yeast *Saccharomyces cerevisiae* (Ynl305c), and other species (Chae et al., 2003). However, when we analyzed the C-terminal sequence of BI-1 from different species, we noticed that the amino acids critical for interaction with IRE1α were not conserved in Ynl305c but were present in other species analyzed (Figure 6A). To assess the function of BI-1 in regulating the UPR in different species in vivo, we first tested the susceptibility of BI-1 KO mice to a stress response. BI-1 mice were treated once with Tm for 6 hr and levels of XBP-1s and ATF4 then analyzed in liver nuclear extracts (Figure 7A). We observed a marked increase of XBP-1s levels in BI-1 KO mice treated with Tm when compared with control animals. However, no differences in the induction of PERK-dependent transcription factor ATF4 were observed. Similar results were observed when XBP-1s levels were monitored in the kidney (Figure 7B).

The IRE1α/XBP-1 branch is highly conserved in *D. melanogaster* (Souid et al., 2007; Plongthongkum et al., 2007). We analyzed the levels of XBP-1 mRNA splicing in flies overexpressing dBI-1. As an experimental model, we grew fly larvae in media containing 50 μg/ml Tm for 20 hr and then measured the levels of XBP-1 mRNA splicing in total tissue extracts, as previously described (Plongthongkum et al., 2007). As shown in Figure 7C, overexpression of dBI-1 significantly decreased the levels of XBP-1 splicing in larvae treated with Tm, indicating that BI-1 also regulates IRE1α in invertebrates. Similar results were observed when dBI-1-overexpressing flies were exposed to thapsigargin or DTT (Figure 7C). Finally, we tested the activity of the putative yeast BI-1 homolog by generating an Yn1305c mutant. Consistent with the lack of conservation of the C-terminal IRE1α-interacting motif, mutant Yn1305c yeast cells did not show any significant increase in levels of the XBP-1 functional homolog HAC1p when compared with control yeast grown in DTT-containing culture media (data not shown), suggesting that while showing some limited amino-acid sequence homology, this yeast protein may not be a close ortholog of BI-1 (S. Bernales, J. Weissman, and P.W., unpublished data).

BI-1 Deficiency Increases ER/Golgi Expansion and Immunoglobulin Secretion in Primary B Cells

Secretory cells require a developed ER for proper function. The first insights about the function of XBP-1 in vivo came from studies in the immune system, where the high demand for immunoglobulin synthesis in B cells constitutes an endogenous source of ER stress (Reimold et al., 2001). XBP-1-deficient B cells are markedly defective in antibody secretion in vivo in response to antigenic challenge (Iwakoshi et al., 2003; Zhang et al., 2005). To evaluate the role of BI-1 in the control of XBP-1-dependent processes in a physiologically relevant system, we determined the rate of IgM secretion in BI-1 KO primary B cells. Increased levels of IgM were observed in the cell-culture media of BI-1-deficient B cells after stimulation with LPS (Figure 7D). This phenomenon was associated with a marked increased staining with Brefeldin A-BODIPY in BI-1 KO cells, which is indicative of an expanded ER and Golgi in these cells compared with controls (Figure 7E), a process previously described to be XBP-1 dependent (Sriburi et al., 2004; Shaffer et al., 2004). Freshly isolated splenic B cells from BI-1 KO mice

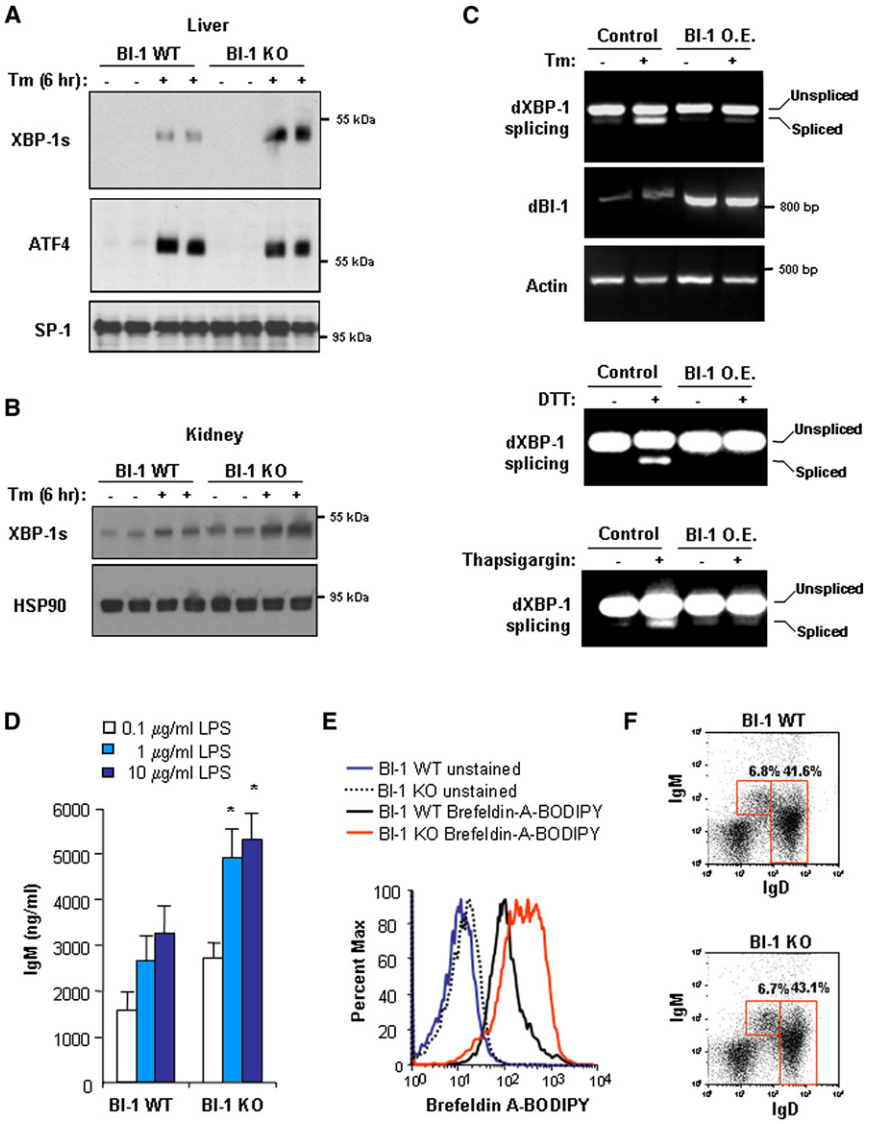

Figure 7. BI-1 Regulates XBP-1 mRNA Splicing In Vivo and Modulates IgM Secretion in Primary B Cells

(A) BI-1 WT and BI-1-deficient mice were injected intraperitoneally with 0.2 μg Tm/g weight, and after 6 hr of treatment, animals were sacrificed and the expression levels of XBP-1 s, ATF4, and SP1 (control) determined by western blot of nuclear extracts from liver.

(B) In parallel, expression of XBP-1 s and HSP90 was determined in kidney total protein extracts from animals presented in (B).

(C) WT or dBI-1 overexpressing *D. melanogaster* larva was grown in the presence or absence of 50 μg/ml Tm, 50 mM DTT, or 10 μM thapsigargin for 20 hr, and levels of XBP-1 splicing were determined by RT-PCR. As control, overexpression levels of dBI-1 mRNA and actin were measured by RT-PCR. Data are representative of three independent experiments.

(D) Shown is a physiological model of ER stress. Primary B cells were purified from spleens of BI-1 WT and KO mice and then stimulated with the indicated concentration of LPS. After 2 days of culture, the levels of IgM were measured in the cell-culture supernatant by ELISA. The values represent the results of the analysis of four different animals. *$p < 0.05$ using Student's t test.

(E) Splenic B cells from BI-1 WT and KO mice were cultured for 2 days in the presence of 0.1 μg/ml LPS, stained with brefeldin A-BODIPY, and then analyzed by FACS to determine relative content of ER and Golgi.

(F) Cell-surface levels of IgM and IgD were measured by FACS analysis of freshly isolated splenocytes from BI-1 WT and KO mice. Average percentages of IgD- and IgM-positive cells are indicated.

showed no differences in surface IgM and IgD expression when compared with control mice (Figure 7F). Taken together, these data indicate that BI-1 regulates two distinct known processes mediated by XBP-1 in primary B cells, ER/Golgi expansion, and immunoglobulin secretion.

DISCUSSION

BI-1 is a specialized and evolutionarily conserved regulator of cell death and is present in species even for which no BCL-2 family homologs have been described including other eukaryotes, plants, bacteria, and even viruses (Chae et al., 2003; Huckelhoven, 2004). Recent studies indicate that several BCL-2 family members reside in other organelles, where they perform novel functions (reviewed in Hetz, 2007). In support of this concept, we recently described that BAX and BAK modulate the stress sensor IRE1α at the ER membrane (Hetz et al., 2006). Here we present evidence indicating that BI-1 negatively regulates the IRE1α/XBP-1 pathway. BI-1-deficient cells showed hyperactivation of IRE1α associated with increased XBP-1 mRNA splicing and upregulation of XBP-1s-dependent responses. Notably, inactivation of IRE1α signaling over time was markedly delayed in BI-1 KO MEFs, indicating an important inhibitory activity of BI-1 on XBP-1 mRNA splicing. This regulation was mediated by the formation of a protein complex between IRE1α and BI-1 and was reconstituted in vitro with purified components. The inhibition of IRE1α by BI-1 was recapitulated in vivo in BI-1-deficient mice and flies overexpressing dBI-1, indicating that this regulation is conserved across species.

Engagement of the IRE1α/XBP-1 pathway confers protection against ER stress (Lin et al., 2007). Our results indicate that BI-1 negatively controls XBP-1s expression, which contrasts with its known general downstream antiapoptotic activity against intrinsic death stimuli (i.e., growth factor deprivation, oxidative stress, and DNA damage) (Xu and Reed, 1998). Interestingly, BI-1's regulatory effects on the UPR are more evident when moderate to low doses of ER stressors are employed, which resembles in vivo conditions in which cells are equipped to

cope with injury (adaptive conditions). In agreement with these findings, we observed an increased rate of IgM secretion in LPS-stimulated BI-1-deficient primary B cells. Consistent with this idea, it has been reported that mild ER stress conditions evoke distinct signaling processes, in which apoptosis-related events are not observed under moderate ER stress (Rutkowski et al., 2006). Our results suggest that the changes in apoptosis observed in BI-1 KO cells may reflect a balance between the inhibition of survival signaling mediated by IRE1α and the general downstream antiapoptotic activity of the intrinsic death machinery (model in Figure S7). Recently, it was reported that BI-1 overexpression may negatively affect ER stress responses through the control of the heme oxygenase-1 gene (Lee et al., 2007). However, we did not observe any effects on the transcription of *Heme Oxygenase-1* in BI-1-deficient MEFs (Figure S6). The regulation of IRE1α by BI-1 may be related to the effects of BAX and BAK on the UPR, where BAX and BAK may compete for a similar binding site on IRE1α. Because BAX and BAK are not present in yeast, the acquisition of UPR modulatory activities may have evolved in higher eukaryotes. In fact, we did not observe a significant effect on the activation of the UPR in Ynl305c-deficient yeast.

Several bifunctional activities for apoptosis-related proteins have been described over the last few years (reviewed in Hetz and Glimcher, 2008a). For example, the proapoptotic protein BAD controls glucose metabolism (Danial et al., 2003) and insulin secretion by β cells (Danial et al., 2008). Similarly, expression of the proapoptotic protein BID is important for engagement of survival DNA repair responses (Zinkel et al., 2005; Kamer et al., 2005). BCL-2-related proteins have inhibitory activities on autophagy, a survival pathway against nutrient starvation (Maiuri et al., 2007; Pattingre et al., 2005). BCL-2 and BCL-X_L also have alternative roles in proinflammatory processes through NALP1 regulation (Bruey et al., 2007). Finally, BAX and BAK were shown to control mitochondrial morphogenesis (Karbowski et al., 2006). Thus, mounting evidence indicates that apoptosis-related proteins have alternative functions and vital roles in normal cellular physiology.

Although PERK and IRE1α share functionally similar luminal sensing domains and are both activated in cells treated with ER stress inducers in vitro, they are selectively activated in vivo by the physiological stress of unfolded proteins. For example, XBP-1 deficiency drastically affects the ability of B lymphocytes to secrete immunoglobulins (Reimold et al., 2001; Iwakoshi et al., 2003; Lee et al., 2005), a defect that is not present in PERK-deficient mice (Gass et al., 2007). The differences in terms of tissue-specific regulation of the UPR in vivo may be explained by the formation of distinct regulatory protein complexes through specific binding of adaptor and modulator proteins. Since several proteins selectively modulate IRE1α signaling (reviewed in Hetz and Glimcher, 2008b), we envision a model in which IRE1α signaling emerges as a more highly regulated process than previously appreciated, and may be controlled by the formation of a complex protein scaffold unto which many other regulatory components assemble (previously referred to as the *UPRosome* [Hetz and Glimcher, 2008b]). Taken together with the current study, increasing evidence suggests a rheostat model in which a balance between anti- and proapoptotic proteins at the ER membrane modulates the amplitude of IRE1α signaling, and hence cellular sensitivity to ER stress conditions.

EXPERIMENTAL PROCEDURES

Materials

Tunicamycin (Tm), brefeldin A, thapsigargin, and zVAD-fmk were purchased from Calbiochem EMB Bioscience Inc. Cell culture media, fetal calf serum, and antibiotics were obtained from Life Technologies (Maryland, USA). Hoechst, LysoTraker, Brefeldin A-BODIPY, and ALEXA secondary antibodies were purchased from Molecular Probes. Anti-IgD and anti-IgM fluorescent antibodies were purchased from BD Biosciences. Peptides were prepared at the Tufts Medical School facility (Boston, MA).

Cell Culture and Constructs

SV40-transformed MEFs were generated and cultured as described (Cheng et al., 2001; Xu and Reed, 1998). HA-tagged IRE1α constructs were previously described (Hetz et al., 2006). In brief, PCR-amplified human IRE1α cDNA was ligated with a linker containing the HA-tag sequences and then inserted into a pMSCV-hygro (Clontech) plasmid between BglII and Xho I sites to generate IRE1α-HA. In addition, IRE1α-(N)-HA containing the amino acid sequences 1–500 or 467–977 of human Ire1α were generated using the same vector. Alternatively, the cytosolic portion of human IRE1α was VSV-tagged using the pCR3 vector. RNase inactive mutant K907A was also generated by site-directed mutagenesis.

Human BI-1 was cloned into pCDNA.3 and MYC tagged as previously described (Xu and Reed, 1998; Chae et al., 2003). Mutants of h-BI-1 were generated by exchanging C-terminal-charged residues for alanine (C9A) using PCR-based methods. The cDNA of hBI-1WT and delta-C mutant were previously cloned (Chae et al., 2003), and we generated EGFP fusion proteins using the pEGFP-N1 vector (Clontech). Then, EGFP fusion proteins were subcloned into pMSCV-puro retroviral vector (Clontech).

Western Blot Analysis

Cells were collected and homogenized in RIPA buffer (20 mM Tris [pH 8.0], 150 mM NaCl, 0.1% SDS, 0.5% DOC, and 0.5% Triton X-100) containing a protease inhibitor cocktail (Roche, Basel, Switzerland) by sonication. To address phosphorylation events, an additional set of phosphatase inhibitors were added to the RIPA buffer (Cocktail I and II, Sigma). Protein concentration was determined by micro-BCA assay (Pierce, Rockford, IL) (Hetz et al., 2003). The equivalent of 30–50 μg of total protein was loaded onto 4%–12%, 7.5%, 12%, or 15% SDS-PAGE minigels (Cambrex) depending on the analysis as described before (Hetz et al., 2005). The following antibodies and dilutions were used: anti-XBP-1 1:1000 (Iwakoshi et al., 2003), anti-GFP 1:1000, anti-HIS-HRP 1:1000, anti-HSP90 1:5000, anti-ATF4 1:2000, anti-eIF2α 1:500, anti-CHOP 1:2000, anti-SP-1 1:1000, anti-BI-1 1:1000 (Santa Cruz, CA), anti-IRE1α 1:1000, anti-BAX 1:2000, anti-BAK 1:2000 (Upstate Technology), and anti-P-eIF2α 1:2000 (Cell Signaling Technology).

RNA Extraction and RT-PCR

Total RNA was prepared from cells placed in cold PBS cells using Trizol (Invitrogen, Carlsbad, CA), and cDNA was synthesized with SuperScript III (Invitrogen, Carlsbad, CA) using random primers $p(dN)_6$ (Roche, Basel, Switzerland). Quantitative real-time PCR reactions employing SYBR green fluorescent reagent were performed in an ABI PRISM 7700 system (Applied Biosystems, Foster City, CA). The relative amounts of mRNAs were calculated from the values of comparative threshold cycle by using β-actin as control. Primer sequences were designed by Primer Express software (Applied Biosystems, Foster City, CA) or obtained from the Primer Data bank (http://pga.mgh.harvard.edu/primerbank/index.html). Real-time PCR was performed as previously described (Lee et al., 2005) using the following primers: *erdj4* 5′-CCCCAGTGTCAAACTGTACCAG-3′ and 5′- AGCGTTTCCAATTTTCCATAAATT-3′; *edem* 5′- AAGCCCTCTGGAA CTTGCG-3′ and 5′-AACCCAATGGCCTGTCTGG-3′; *sec61a* 5′-CTATTTC CAGGGCTTCCGAGT-3′ and 5′-AGGTGTTGTACTGGCCTCGGT-3′; *herp* 5′- CATGTACCTGCACCACGTCG-3′ and 5′-GAGGACCACCATCATCCGG-3′; *actin* 5′- TACCACCATGTACCCAGGCA-3′ and 5-′CTCAGGAGGAGCAA

TGATCTTGAT-3′; *wfs-1* 5′-CCATCAACATGCTCC CGTTC-3′ and 5′-GGGT AGGCCTCGCCAT-3′; *xbp-1* 5′-CCTGAGCCCGGAGGAGAA-3′ and 5′-CTCGA GCAGTCTGCGCTG-3′; *HO1* 5′-CACAGCACTATGTAAAGCGTCT-3′ and 5′-TGTGCAATCTTCTTCAGGACC-3′; *ero1* TCAGTGGACCAAGCATGATGA-3′ and 5′-TCCACATACTCAGCATCGGG-3′ ; *bi-1* 5′-GACCGAGCAAAAGAGAC TGG-3′ and 5′-AAGGCCAGGATCAACATGAG-3′; and *xbp-1 s* 5′-GAGTCCG CAGCAGGTG-3′ and 5′-GTGTCAGAGTCCATGGGA-3′.

XBP-1 mRNA Splicing Assay

XBP-1 mRNA splicing assay was performed as previously described (Lee et al., 2003b; Iwakoshi et al., 2003). In brief, PCR primers 5′-ACACGCTTGG GAATGGACAC-3′ and 5′-CCATGGGAAGA TGTTCTGGG-3′ encompassing the spliced sequences in xbp-1 mRNA were used for the PCR amplification with AmpliTaq Gold polymerase (Applied Biosystem, Foster City, CA). We separated the PCR products by electrophoresis on a 2.5% agarose gel (Agarose-1000 Invitrogen, Carlsbad, CA) and visualized them by ethidium bromide staining. XBP-1's mRNA stability was monitored using the conditions described in (Hollien and Weissman, 2006) and quantification by real-time PCR.

Knockdown of BI-1, IRE1α, and XBP-1

We generated stable MEFs with reduced levels of BI-1 using methods previously described (Hetz et al., 2007) by targeting BI-1 mRNA with shRNA using the lentiviral expression vector pLKO.1 and puromycin selection. As control, a shRNA against the *luciferase* gene was employed. Constructs were generated by The Broad Institute (Boston, MA) based on different criteria for shRNA design (see http://www.broad.mit.edu/genome_bio/trc/rnai.html). We screened for each gene a total of five different constructs and selected the most efficient construct for the analysis. Targeting sequences identified for mouse BI-1, XBP-1 and IRE1α were 5′-CCTCTTTGATACTCAGCTCAT-3′, 5′-CCATTAAT GAACTCATTCGTT-3′, and 5′-GCTCGTGAATTGATAGAGAAA-3′, respectively.

Immunoprecipitations and Pull-Down Assay

Immunoprecipitations (IP) were conducted in CHAPS buffer (1% CHAPS, 100 mM KCl, 50 mM Tris [pH 7.5], 50 mM NaF, 1 mM Na3VO4, 250 mM PMSF, and protease inhibitors). For the preparation of cell extracts, cells were collected in PBS, resuspended in CHAPS buffer, and incubated at 4°C for 30 min in a wheel rotor. IP was performed in 500 μl of postnuclear extracts containing 750 μg protein. Cleared extracts were incubated with the antibody-protein A/G complex (Santa Cruz), anti-HA antibody-agarose complexes (Roche), or anti-MYC antibody-agarose complexes (Upstate Technology) for 4 hr at 4°C, and then washed twice in 1 ml of CHAPS buffer and then one time in CHAPS buffer with 500 mM NaCl. Protein complexes were eluted by boiling in SDS sample buffer or by competing with 1.4 mg/ml HA peptide (Roche) or MYC peptide (Upstate Technology) for 30 min at 4°C and then 10 min at 37°C.

For the BI-1 peptide competition assay, BI-1-MYC and IRE1-VSV were coexpressed in HEK cells and BI-1 was immunoprecipitated with anti-MYC agarose. Immunoprecipitated protein complexes were incubated in CHAPS buffer with BI-$1^{C\text{-}ter}$ or control peptides for 30 min at room temperature and then washed twice with CHAPS buffer. Then, BI-1-MYC/IRE1-VSV complexes were eluted from the anti-MYC-agarose with a synthetic MYC peptide as described above and analyzed by western blot. The BI-1 peptide sequence was RRRRRRRRLAMNEKDKKKEKK (BI-$1^{C\text{-}ter}$) or control peptide RRRRRRRRKEKMKLKANKEDK (scrambled).

Production of recombinant IRE1ΔN-HIS insect cells was previously described (Hetz et al., 2006). IVTT proteins were prepared according to the recommendations of the manufacturer (Promega) and labeled with 10 μ curie of Met-^{35}S per reaction during synthesis (Easy Tag Methionine-[^{35}S], Perkin Elmer). Pull-down assays with recombinant proteins were performed in CHAPS buffer. Ten micrograms of IRE1ΔN-HIS was incubated with 20 μl of IVTT BI-1-MYC (cloned in pCDNA.3 vector) in a total volume of 250 μl of CHAPS buffer containing 0.1% BSA for 3 hr at 4°C, and then, protein complexes were captured with 20 μl anti-HIS agarose for 2 hr at 4°C (Santa Cruz). After four washes in CHAPS buffer, bound proteins were eluted by incubating the proteins at 37°C for 10 min in SDS sample buffer prepared with RIPA buffer and 1 mM urea and then analyzed by western blot or autoradiography. Alternatively, to test the effects of BI-1 on the binding of BAX to IRE1α, 40 μl of radiolabeled IVTT BAX (cloned into pCDNA.3) was introduced in the same experiment using unlabeled BI-1 and then analyzed by pull-down assays as described above.

In Vitro IRE1α Activity Assays

The activity of recombinant human IRE1ΔN-HIS was monitored in vitro because this deletion mutant adopts a dimeric active structure as measured by nondenaturing electrophoresis and silver staining (data not shown). IRE1ΔN-HIS was incubated with 20 μl of IVTT BI-1-MYC in a total volume of 100 μl for 1 hr at 30°C. As control, an IVTT reaction was prepared with pCDNA.3 empty vector. Then, the protein mix was incubated for 1 hr at 30°C with 10 μg of total mRNA as substrate (obtained from mouse brain cortex because of minimal basal XBP-1 mRNA splicing levels) in a buffer containing 20 mM HEPES (pH 7.3), 1 mM DTT, 10 mM magnesium acetate, 50 mM potassium acetate, and 2 mM ATP. Then, mRNA was re-extracted with 500 μl of Trizol, and the endoribonuclease activity of IRE1α was monitored by RT-PCR using the XBP-1 mRNA splicing assay that employs a set of primers that closely surround the processing site. Using this method, we observed a decrease in the amount of nonspliced XBP-1 mRNA due to its cleavage by IRE1ΔN-HIS as previously described by with an alternative in vitro splicing assay (Calfon et al., 2002). As control, total XBP-1 mRNA (a fragment not affected by the processing) and actin levels were monitored.

Alternatively, IRE1α-HA was immunoprecipitated from BI-1 WT and KO MEFs from a 10 cm plate as described above. Then, protein complexes were incubated for 1 hr at 30°C with 10 μg of total mRNA in the endoribonuclease reaction described above. Using this method, we obtained spontaneous splicing activity possible due to artificial dimerization by antibody cross-linking. Of note, in addition to detect the ribonuclease activity of IRE1α, we observed a ligation process associated with the appearance of XBP-1's PCR fragment. We speculate that since our immunoprecipitations are done under nondenaturing conditions, the IRE1-containing protein complexes may contain the ligase activity.

Fluorescent Labeling

Lysosomes, mitochondria, or ER/Golgi were visualized using specific fluorescent probes. Living cells were stained with 200 nM LysoTraker or MitoTracker for 45 min at 37°C and 5% CO2. ER/Golgi was visualized by 0.2 μg/ml of Brefeldin A-BODIPY for 45 min by adding it directly to the medium. Cells were washed two times with cold PBS and then fixed for 30 min with 4% formaldehyde on ice. Then cells were maintained in PBS containing 0.4% formaldehyde for visualization on a confocal microscope.

MYC-tagged proteins were visualized by immunofluorescence. Cells were fixed for 30 min in PBS containing 4% paraformaldehyde and permeabilized with cold methanol at 20°C for 10 min. After blocking for 1 hr with 5% gelatin, cells were subsequently incubated with anti-calnexin or anti-MYC antibodies for 1 hr at 37°C, washed three times in PBS, and incubated with Alexa-conjugated secondary antibodies (Molecular Probes) for analysis on a confocal microscope. Nuclei were stained with Hoechst dye.

In Vivo Mouse Experiments

Animals were given a single 0.2 μg/gram body weight intraperitoneal injection of a 0.05 mg/ml suspension of Tm in 150 mM dextrose as previously described (Hetz et al., 2006). After 6 hr, mice were killed by CO2 narcosis. Livers and kidneys were removed, and protein extracts were prepared for western blot analysis. For analysis of XBP-1 in liver samples, cell extracts were fractionated into nuclear fractions as previously described with minor modifications (Hetz et al., 2006). Kidney extracts were prepared by sonication in RIPA buffer.

B Cell Experiments

Single-cell suspensions of splenocytes were prepared from BI-1 WT or KO mice, and red blood cells were removed by ammonium chloride lysis. A fraction of splenocytes were stained with fluorochrome-conjugated anti-IgM and anti-IgD antibodies for FACS analysis. Remaining splenocytes were used for the isolation of B cells by $B220^{+}$ magnetic bead selection (Miltenyi Biotec, Auburn, CA). Purified B cells were cultured in complete medium containing

RPMI 1640 supplemented with 10% fetal bovine serum, 2 mM glutamine, 50 units/ml penicillin, 50 μg/ml streptomycin, 100 mM HEPES, 1× nonessential amino acids, 1 mM sodium pyruvate, 50 μM β-mercaptoethanol, and stimulated with 0.1, 1.0, or 10 μg/ml LPS (Sigma, St. Louis, MO). Cells and supernatants were harvested at day 2 of culture. Cells were stained with Brefeldin A BODIPY, as described above, washed, and analyzed immediately by FACS for ER/Golgi content. Controls to monitor correct staining of the ER by brefeldin A-BODIPY were previously described (Hetz et al., 2006; Shaffer et al., 2004). IgM was measured in supernatants by ELISA as described (Reimold et al., 2001).

Yeast Strains

Strains used in this study were generated from the wild-type strain w303. Strain Δynl305c was produced using PCR-based knockout strategy (Longtine et al., 1998). Cells were grown in YPD media or in defined synthetic medium at 30°C to logarithmic phase. When necessary, 8 mM dithiothreitol (DTT), 0.2 mM and 1.0 mM tunicamycin, and media deficient in inositol were used to induce the UPR. To detect pHac levels in control and Δynl305c strains, protein lysates were prepared using urea buffer, and protein concentration was determined by the Bradford assay (Bio-Rad Protein Assay, Hercules, CA). Fifty micrograms of total protein for each sample was loaded onto NuPAGE 10% Bis-Tris Gels (Invitrogen, Carlsbad, CA), to then be analyzed by western blotting technique. pHac1 was detected using a polyclonal anti-HA antibody (Cox and Walter, 1996); as a loading control, monoclonal antibody against PGK (Invitrogen 22C5) was used at 1:5000.

Fly Stocks and Tunicamycin Treatments

The dBI-1^{EY03662} mutant fly corresponds to a single P element inserted in the 5′ UTR, 63 bp downstream of the dBI-1 (CG7188) transcription start site. This insertion produces the overexpression of dBI-1 as detected by real-time RT-PCR. For UPR assays, Canton S and dBI-1^{EY03662} larvae were grown in standard media or standard media supplemented with 50 μg/ml tunicamycin, 10 μM thapsigargin, or 50 mM DTT for 20 hr, and total RNA was extracted and dXbp-1 splicing analyzed. A total of 15 larvae were pulled for each experiment. The dBI-1^{EY03662} fly was obtained from the Bloomington stock center (BL-16568).

Statistical Analysis

Data were analyzed by Student's t test or two-way ANOVA when groups of data were analyzed. The GraphPad Prism 5 software was employed for statistical analysis.

SUPPLEMENTAL DATA

The Supplemental Data include seven figures and can be found with this article online at http://www.cell.com/molecular-cell/supplemental/S1097-2765(09)00133-6.

ACKNOWLEDGMENTS

We thank Drs. Alfred Zullo, Sebastian Bernales, Han Li, and Ann-Hwee Lee for helpful discussions and Gabriela Martinez and Jennifer Donovan for technical assistance. We thank Jonathan Weissman and Sebastian Bernales for performing yeast experiments, Dr. Nir Hacohen and The Broad Institute (Cambidge, MA) for providing the shRNA constructs, Dr. Josef Opherman for providing MCL-1-deficient cells, and Dr. Nika Danial for providing BAX and BAK DKO and BCL-2 KO cells. This work was supported by the V. Harold and Leila Y. Mathers Charitable Foundation (L.H.G.), NIHAI32412 (L.H.G.); FONDECYT number 1070444, FONDAP grant number 15010006, Millennium Nucleus number P07-048-F, The Muscular Dystrophy Association, The Michael J. Fox Foundation for Parkinson's Research, National Parkinson's Disease, and High Q Foundation (C.H.); CONICYT fellowship (D.R.-R.); ICM P06-039 (A.G.); AI-15353 (J.C.R.); and grants from the National Institutes of Health and the U.S. Department of Defense (P.W.). P.W. is an Investigator of the Howard Hughes Medical Institute. L.H.G. has equity in and is on the Corporate Board of Directors of the Bristol-Myers Squibb Company.

Received: September 10, 2008
Revised: December 30, 2008
Accepted: February 16, 2009
Published: March 26, 2009

REFERENCES

Acosta-Alvear, D., Zhou, Y., Blais, A., Tsikitis, M., Lents, N.H., Arias, C., Lennon, C.J., Kluger, Y., and Dynlacht, B.D. (2007). XBP1 controls diverse cell type- and condition-specific transcriptional regulatory networks. Mol. Cell *27*, 53–66.

Bailly-Maitre, B., Fondevila, C., Kaldas, F., Droin, N., Luciano, F., Ricci, J.E., Croxton, R., Krajewska, M., Zapata, J.M., Kupiec-Weglinski, J.W., et al. (2006). Cytoprotective gene bi-1 is required for intrinsic protection from endoplasmic reticulum stress and ischemia-reperfusion injury. Proc. Natl. Acad. Sci. USA *103*, 2809–2814.

Bruey, J.M., Bruey-Sedano, N., Luciano, F., Zhai, D., Balpai, R., Xu, C., Kress, C.L., Bailly-Maitre, B., Li, X., Osterman, A., et al. (2007). Bcl-2 and Bcl-XL regulate proinflammatory caspase-1 activation by interaction with NALP1. Cell *129*, 45–56.

Calfon, M., Zeng, H., Urano, F., Till, J.H., Hubbard, S.R., Harding, H.P., Clark, S.G., and Ron, D. (2002). IRE1 couples endoplasmic reticulum load to secretory capacity by processing the XBP-1 mRNA. Nature *415*, 92–96.

Chae, H.J., Ke, N., Kim, H.R., Chen, S., Godzik, A., Dickman, M., and Reed, J.C. (2003). Evolutionarily conserved cytoprotection provided by Bax Inhibitor-1 homologs from animals, plants, and yeast. Gene *323*, 101–113.

Chae, H.J., Kim, H.R., Xu, C., Bailly-Maitre, B., Krajewska, M., Krajewski, S., Banares, S., Cui, J., Digicaylioglu, M., Ke, N., et al. (2004). BI-1 regulates an apoptosis pathway linked to endoplasmic reticulum stress. Mol. Cell *15*, 355–366.

Cheng, E.H., Wei, M.C., Weiler, S., Flavell, R.A., Mak, T.W., Lindsten, T., and Korsmeyer, S.J. (2001). BCL-2, BCL-X(L) sequester BH3 domain-only molecules preventing BAX- and BAK-mediated mitochondrial apoptosis. Mol. Cell *8*, 705–711.

Cox, J.S., and Walter, P. (1996). A novel mechanism for regulating activity of a transcription factor that controls the unfolded protein response. Cell *87*, 391–404.

Danial, N.N., and Korsmeyer, S.J. (2004). Cell death: critical control points. Cell *116*, 205–219.

Danial, N.N., Gramm, C.F., Scorrano, L., Zhang, C.Y., Krauss, S., Ranger, A.M., Datta, S.R., Greenberg, M.E., Licklider, L.J., Lowell, B.B., et al. (2003). BAD and glucokinase reside in a mitochondrial complex that integrates glycolysis and apoptosis. Nature *424*, 952–956.

Danial, N.N., Walensky, L.D., Zhang, C.Y., Choi, C.S., Fisher, J.K., Molina, A.J., Datta, S.R., Pitter, K.L., Bird, G.H., Wikstrom, J.D., et al. (2008). Dual role of proapoptotic BAD in insulin secretion and beta cell survival. Nat. Med. *14*, 144–153.

Gass, J.N., Jiang, H.Y., Wek, R.C., and Brewer, J.W. (2007). The unfolded protein response of B-lymphocytes: PERK-independent development of antibody-secreting cells. Mol. Immunol. *45*, 1035–1043.

Gu, F., Nguyen, D.T., Stuible, M., Dube, N., Tremblay, M.L., and Chevet, E. (2004). Protein-tyrosine phosphatase 1B potentiates IRE1 signaling during endoplasmic reticulum stress. J. Biol. Chem. *279*, 49689–49693.

Hetz, C.A. (2007). ER stress signaling and the BCL-2 family of proteins: from adaptation to irreversible cellular damage. Antioxid. Redox Signal. *9*, 2345–2356.

Hetz, C., and Glimcher, L. (2008a). The daily job of night killers: alternative roles of the BCL-2 family in organelle physiology. Trends Cell Biol. *18*, 38–44.

Hetz, C., and Glimcher, L. (2008b). The UPRosome and XBP-1: mastering secretory cell function. Curr. Immunol. Rev. *4*, 1–10.

Hetz, C., Russelakis-Carneiro, M., Maundrell, K., Castilla, J., and Soto, C. (2003). Caspase-12 and endoplasmic reticulum stress mediate neurotoxicity of pathological prion protein. EMBO J. *22*, 5435–5445.

Hetz, C., Russelakis-Carneiro, M., Walchli, S., Carboni, S., Vial-Knecht, E., Maundrell, K., Castilla, J., and Soto, C. (2005). The disulfide isomerase Grp58 is a protective factor against prion neurotoxicity. J. Neurosci. *25*, 2793–2802.

Hetz, C., Bernasconi, P., Fisher, J., Lee, A.H., Bassik, M.C., Antonsson, B., Brandt, G.S., Iwakoshi, N.N., Schinzel, A., Glimcher, L.H., and Korsmeyer, S.J. (2006). Proapoptotic BAX and BAK modulate the unfolded protein response by a direct interaction with IRE1alpha. Science *312*, 572–576.

Hetz, C., Thielen, P., Fisher, J., Pasinelli, P., Brown, R.H., Korsmeyer, S., and Glimcher, L. (2007). The proapoptotic BCL-2 family member BIM mediates motoneuron loss in a model of amyotrophic lateral sclerosis. Cell Death Differ. *14*, 1386–1389.

Hollien, J., and Weissman, J.S. (2006). Decay of endoplasmic reticulum-localized mRNAs during the unfolded protein response. Science *313*, 104–107.

Huckelhoven, R. (2004). BAX Inhibitor-1, an ancient cell death suppressor in animals and plants with prokaryotic relatives. Apoptosis *9*, 299–307.

Iwakoshi, N.N., Lee, A.H., Vallabhajosyula, P., Otipoby, K.L., Rajewsky, K., and Glimcher, L.H. (2003). Plasma cell differentiation and the unfolded protein response intersect at the transcription factor XBP-1. Nat. Immunol. *4*, 321–329.

Kamer, I., Sarig, R., Zaltsman, Y., Niv, H., Oberkovitz, G., Regev, L., Haimovich, G., Lerenthal, Y., Marcellus, R.C., and Gross, A. (2005). Proapoptotic BID is an ATM effector in the DNA-damage response. Cell *122*, 593–603.

Karbowski, M., Norris, K.L., Cleland, M.M., Jeong, S.Y., and Youle, R.J. (2006). Role of Bax and Bak in mitochondrial morphogenesis. Nature *443*, 658–662.

Lee, K., Tirasophon, W., Shen, X., Michalak, M., Prywes, R., Okada, T., Yoshida, H., Mori, K., and Kaufman, R.J. (2002). IRE1-mediated unconventional mRNA splicing and S2P-mediated ATF6 cleavage merge to regulate XBP1 in signaling the unfolded protein response. Genes Dev. *16*, 452–466.

Lee, A.H., Iwakoshi, N.N., and Glimcher, L.H. (2003a). XBP-1 regulates a subset of endoplasmic reticulum resident chaperone genes in the unfolded protein response. Mol. Cell. Biol. *23*, 7448–7459.

Lee, A.H., Iwakoshi, N.N., Anderson, K.C., and Glimcher, L.H. (2003b). Proteasome inhibitors disrupt the unfolded protein response in myeloma cells. Proc. Natl. Acad. Sci. USA *100*, 9946–9951.

Lee, A.H., Chu, G.C., Iwakoshi, N.N., and Glimcher, L.H. (2005). XBP-1 is required for biogenesis of cellular secretory machinery of exocrine glands. EMBO J. *24*, 4368–4380.

Lee, G.H., Kim, H.K., Chae, S.W., Kim, D.S., Ha, K.C., Mike, C., Kress, C., Reed, J.C., Kim, H.R., and Chae, H.J. (2007). Bax inhibitor-1 regulates endoplasmic reticulum stress-associated reactive oxygen species and heme oxygenase-I expression. J. Biol. Chem. *282*, 21618–21628.

Lee, A.H., Scapa, E.F., Cohen, D.E., and Glimcher, L.H. (2008). Regulation of hepatic lipogenesis by the transcription factor XBP1. Science *320*, 1492–1496.

Lin, J.H., Li, H., Yasumura, D., Cohen, H.R., Zhang, C., Panning, B., Shokat, K.M., Lavail, M.M., and Walter, P. (2007). IRE1 signaling affects cell fate during the unfolded protein response. Science *318*, 944–949.

Longtine, M.S., McKenzie, A., III, Demarini, D.J., Shah, N.G., Wach, A., Brachat, A., Philippsen, P., and Pringle, J.R. (1998). Additional modules for versatile and economical PCR-based gene deletion and modification in Saccharomyces cerevisiae. Yeast *14*, 953–961.

Luo, D., He, Y., Zhang, H., Yu, L., Chen, H., Xu, Z., Tang, S., Urano, F., and Min, W. (2008). AIP1 is critical in transducing IRE1-mediated endoplasmic reticulum stress response. J. Biol. Chem. *283*, 11905–11912.

Maiuri, M.C., Le, T.G., Criollo, A., Rain, J.C., Gautier, F., Juin, P., Tasdemir, E., Pierron, G., Troulinaki, K., Tavernarakis, N., et al. (2007). Functional and physical interaction between Bcl-X(L) and a BH3-like domain in Beclin-1. EMBO J. *26*, 2527–2539.

Pattingre, S., Tassa, A., Qu, X., Garuti, R., Liang, X.H., Mizushima, N., Packer, M., Schneider, M.D., and Levine, B. (2005). Bcl-2 antiapoptotic proteins inhibit Beclin 1-dependent autophagy. Cell *122*, 927–939.

Plongthongkum, N., Kullawong, N., Panyim, S., and Tirasophon, W. (2007). Ire1 regulated XBP1 mRNA splicing is essential for the unfolded protein response (UPR) in Drosophila melanogaster. Biochem. Biophys. Res. Commun. *354*, 789–794.

Reimold, A.M., Iwakoshi, N.N., Manis, J., Vallabhajosyula, P., Szomolanyi-Tsuda, E., Gravallese, E.M., Friend, D., Grusby, M.J., Alt, F., and Glimcher, L.H. (2001). Plasma cell differentiation requires the transcription factor XBP-1. Nature *412*, 300–307.

Ron, D., and Walter, P. (2007). Signal integration in the endoplasmic reticulum unfolded protein response. Nat. Rev. Mol. Cell Biol. *8*, 519–529.

Rutkowski, D.T., Arnold, S.M., Miller, C.N., Wu, J., Li, J., Gunnison, K.M., Mori, K., Sadighi Akha, A.A., Raden, D., and Kaufman, R.J. (2006). Adaptation to ER stress is mediated by differential stabilities of pro-survival and pro-apoptotic mRNAs and proteins. PLoS Biol. *4*, e374. 10.1371/journal.pbio.0040374.

Shaffer, A.L., Shapiro-Shelef, M., Iwakoshi, N.N., Lee, A.H., Qian, S.B., Zhao, H., Yu, X., Yang, L., Tan, B.K., Rosenwald, A., et al. (2004). XBP1, downstream of Blimp-1, expands the secretory apparatus and other organelles, and increases protein synthesis in plasma cell differentiation. Immunity *21*, 81–93.

Souid, S., Lepesant, J.A., and Yanicostas, C. (2007). The xbp-1 gene is essential for development in Drosophila. Dev. Genes Evol. *217*, 159–167.

Sriburi, R., Jackowski, S., Mori, K., and Brewer, J.W. (2004). XBP1: a link between the unfolded protein response, lipid biosynthesis, and biogenesis of the endoplasmic reticulum. J. Cell Biol. *167*, 35–41.

Xu, Q., and Reed, J.C. (1998). Bax inhibitor-1, a mammalian apoptosis suppressor identified by functional screening in yeast. Mol. Cell *1*, 337–346.

Zhang, K., Wong, H.N., Song, B., Miller, C.N., Scheuner, D., and Kaufman, R.J. (2005). The unfolded protein response sensor IRE1alpha is required at 2 distinct steps in B cell lymphopoiesis. J. Clin. Invest. *115*, 268–281.

Zinkel, S.S., Hurov, K.E., Ong, C., Abtahi, F.M., Gross, A., and Korsmeyer, S.J. (2005). A role for proapoptotic BID in the DNA-damage response. Cell *122*, 579–591.